Naval Research Laboratory

NRL Report 9119

AD-A196 232

Track Performance Considerations
for Monopulse Radars

CHING-TAI LIN

Search Radar Branch
Radar Division

DEAN D. HOWARD

Locus, Inc.
Alexandria, VA

June 8, 1988

DTIC
SELECTED
JUL 1 3 1988
D

88   729

REPORT DOCUMENTATION PAGE

1a REPORT SECURITY CLASSIFICATION UNCLASSIFIED		1b RESTRICTIVE MARKINGS			
2a SECURITY CLASSIFICATION AUTHORITY		3 DISTRIBUTION / AVAILABILITY OF REPORT Approved for public release; distribution unlimited.			
2b DECLASSIFICATION / DOWNGRADING SCHEDULE					
4 PERFORMING ORGANIZATION REPORT NUMBER(S) NRL Report 9119		5 MONITORING ORGANIZATION REPORT NUMBER(S)			
6a NAME OF PERFORMING ORGANIZATION Naval Research Laboratory	6b OFFICE SYMBOL (If applicable) Code 5333	7a NAME OF MONITORING ORGANIZATION			
6c ADDRESS (City, State, and ZIP Code) Washington, DC 20375-5000		7b ADDRESS (City, State, and ZIP Code)			
8a NAME OF FUNDING / SPONSORING ORGANIZATION Naval Air Development Center	8b OFFICE SYMBOL (If applicable)	9 PROCUREMENT INSTRUMENT IDENTIFICATION NUMBER			
8c ADDRESS (City, State, and ZIP Code) Warminster, PA 18974-5000		10 SOURCE OF FUNDING NUMBERS			

PROGRAM ELEMENT NO	PROJECT NO	TASK NO	WORK UNIT ACCESSION NO
62113N	R13210000	RS34-372-000 WF34-372-000	DN980-327

11 TITLE (Include Security Classification)

Track Performance Considerations for Monopulse Radars

12 PERSONAL AUTHOR(S)
Lin, C.T. and Howard, D.D.

13a. TYPE OF REPORT	13b. TIME COVERED FROM 8/87 TO 1/88	14. DATE OF REPORT (Year, Month, Day) 1988 June 8	15 PAGE COUNT 26

16 SUPPLEMENTARY NOTATION

17 COSATI CODES			18. SUBJECT TERMS (Continue on reverse if necessary and identify by block number)
FIELD	GROUP	SUB-GROUP	Monopulse radar

19 ABSTRACT (Continue on reverse if necessary and identify by block number)

A generic monopulse radar simulation model is being developed to assess the effectiveness of counter-measures and counter-countermeasures in selectable tactical scenarios. In this report, track performance consideration for monopulse radars is analyzed in detail. The radar tracking stability and sensitivity are analyzed in terms of the open-loop gain crossover, open-loop phase margin, and the closed-loop bandwidth and damping ratio. Track loops are synthesized through filter pole/zero placement with consideration of the overall loop gain. An analytical solution is derived as a function of radar parameters that describes the angle and range tracking responses. This eliminates time-consuming computer simulations and provides detailed insight into how basic radar characteristics affect monopulse radar track.

20 DISTRIBUTION / AVAILABILITY OF ABSTRACT ☒ UNCLASSIFIED/UNLIMITED ☐ SAME AS RPT. ☐ DTIC USERS	21. ABSTRACT SECURITY CLASSIFICATION UNCLASSIFIED	
22a NAME OF RESPONSIBLE INDIVIDUAL Dr. C.T. Lin	22b TELEPHONE (Include Area Code) (202) 767-6947	22c. OFFICE SYMBOL Code 5333

DD FORM 1473, 84 MAR

i

CONTENTS

TRACK PERFORMANCE CONSIDERATIONS
FOR MONOPULSE RADARS

INTRODUCTION

A tracking radar typically measures target azimuth and elevation relative to its antenna beam axis and time of arrival of its echo relative to a range tracking gate. This information is used to close tracking loops to cause its antenna beam to follow the target in angle and its range gate to follow the echo arrival time. Monopulse radars can perform this task with very high precision. However, the precision is limited because the targets have finite size with multiple reflecting surfaces causing glint; the radars operate in natural environments with clutter and multipath; and the radars, in tactical scenarios, are exposed to active and passive countermeasures. The wide variety of sources of error, particularly when occurring simultaneously, is difficult to analyze or measure. The performance determination is even more difficult when the radar equipment is not available, or may not exist, and only system parameters are known. A generic tracking radar model is being developed to provide realistic tracking performance by a selectable monopulse system tracking a finite-size complex target in natural and countermeasure enviroments. The model is adaptable to a variety of monopulse radar configurations.

Assessment of radar track performance, such as loss of track because of imperfections in the radar system design, target scintillation, multipath fading, or effects of countermeasures (CM) can be obtained as long as these parameters are included in the simulation. These modeling and synthesizing processes are, however, time-consuming. In parallel with the development of a generic tracking radar simulator, a theoretical analysis of track performance of monopulse radars is reported here.

The study validates results of model simulation and also provides detailed insight into how basic radar characteristics affect monopulse radar track. The radar tracking stability and sensitivity are analyzed in terms of the open-loop gain crossover, phase margin, closed-loop bandwidth, damping ratio, and natural oscillation frequency. Track loops are synthesized through filter pole/zero placement with consideration of the overall loop gain. Bode and Nyquist plots and closed-loop responses are obtained as part of the measure of track performance. A closed-form solution of the radar track in response to a step error input is analytically derived. Fundamental radar track performance can thus be observed without complex model simulation.

MONOPULSE RADAR

The basic three-channel (sum, azimuth-difference, and elevation-difference) monopulse tracking technique [1], as shown in Fig. 1, is used for the development of a generic tracking radar simulator [1]. A typical model simulation is shown in Fig. 2. This model includes the schematic RF feed, the combining circuit of a four-horn monopulse comparator, a three-channel linear IF receiver with automatic gain control (AGC), an integrating sample-and-hold following a dot-product detector and a low-pass filter, and a range tracker using an early-late gate range discriminator. The finite-size complex target is modeled by a collection of scatterers having different magnitudes and varying phase
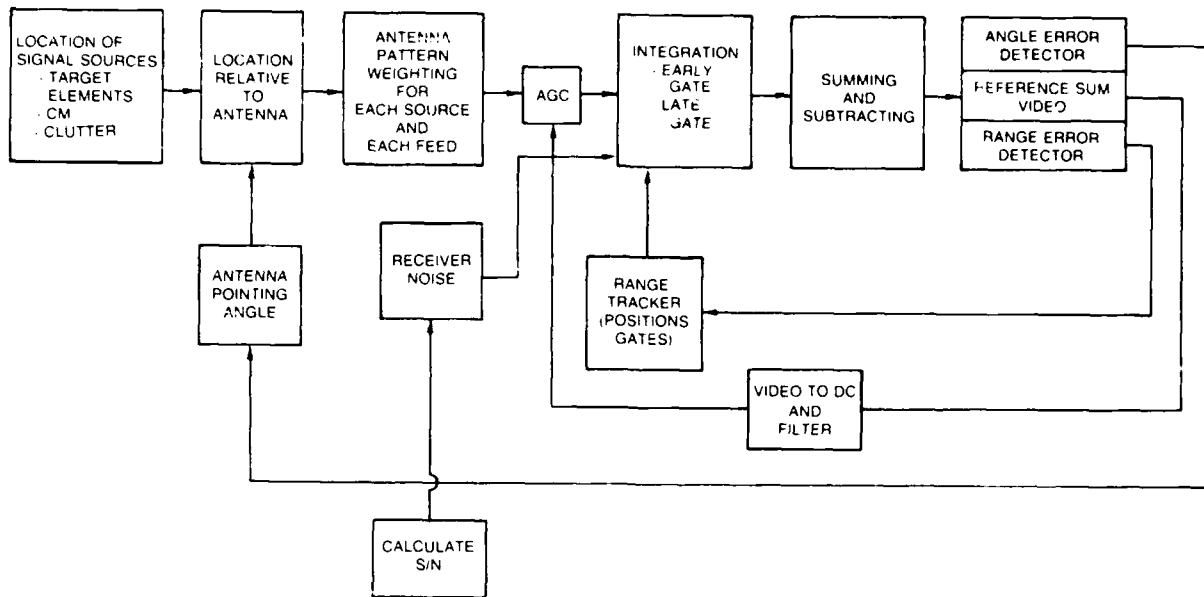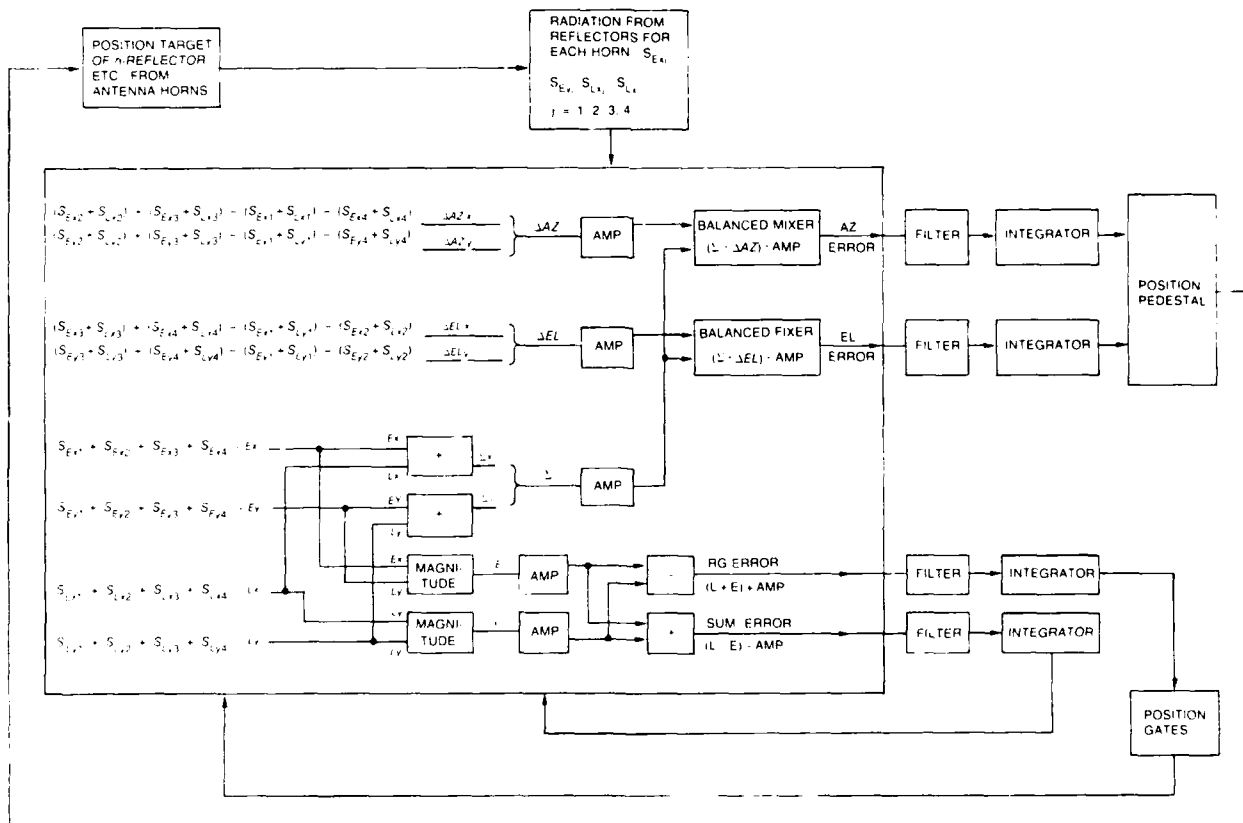

1

Fig. 1 — Monopulse radar modeling

Fig. 2 — A typical monopulse radar simulator

rates. Chaff is formed by a patch of reflectors in different scenarios. The standoff jammers are, however, modeled by scatterers collocated in azimuth and elevation but having random phases and Raleigh-distributed magnitudes that are independent of their ranges to the radar.

The generic tracking radar simulator is sufficiently detailed to provide selection of a wide variety of antenna feeds with responses to both normal and cross-polarized signals, complex targets with selectable size and configuration, low-angle multipath, standoff jammers, basic chaff, and expendable towed and forward-fired decoys. For example, Fig. 3 shows the elevation and azimuth tracking and the receiver gain for a a complex target under the environment of zero-state multipath. Here a low-altitude track is occurring with a monopulse radar of ~0.7° beamwidth. Figure 4 shows the angle and range tracks for towed expendable CM tracking. In this case, a simple level flight path is used, and the jammer is turned on at 24,000 yd and turned off at 15,000 yd. The towed expendable is assumed to be 200 yd behind the target, with repeated pulses at 300 and 400 yd behind the target. Breaking radar track during jammer radiation is clearly shown in the figure.

ANGLE-ERROR SENSITIVITY

Figure 2 shows that the monopulse error voltages entering the shaping filters are prominently affected by the angle error detectors and are characterized by the antenna sum-and-difference patterns. To have a stable closed-loop servo system on angle track, the angle sensitivity must be independent of the target size and range. In the present configuration this is accomplished by AGC with a voltage proportional to the sum channel IF output to control the overall loop gain in three receiver channels. Other monopulse processors with instantaneous AGC by use of a log detector can also be implemented. In practice, the angle error voltage is not exactly linear with respect to the angle error. Typically, a linear relation with a best fit to the actual radar characteristic is assumed. Figure 5 is an example of measured data showing two linear approximations that may be selected depending on the range of off-axis angles to be corrected.

From the basic radar equation, the received signal power is

$$P_s = k \frac{P_t G_T G_R \sigma(t) \lambda^2}{(4\pi)^3 R(t)^4},$$ (1)

where

P_t is transmit power,

G_T is transmitted antenna power gain,

$R(t)$ is range to the target,

G_R is received antenna power gain,

$\sigma(t)$ is target scattering cross section,

λ is wavelength, and

k is a constant.

Let Σ and Δ be the antenna sum-pattern and difference-pattern voltage gains, respectively. Assume that they are proportional to the square roots of the antenna sum-pattern and difference-pattern power gains. Then, the sum and difference signals at the radar IF output are, respectively,

$$\hat{V}_s = k \Sigma^2 \sqrt{P_t \sigma(t)}/R^2(t) \text{ and } \hat{V}_D = k \Sigma \Delta \sqrt{P_t \sigma(t)}/R^2(t),$$
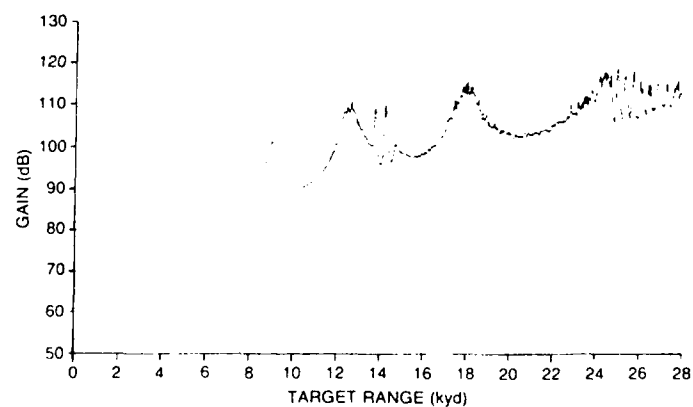
where k is a constant. This is time variant since the target-scattering cross section and the range to target are functions of time.
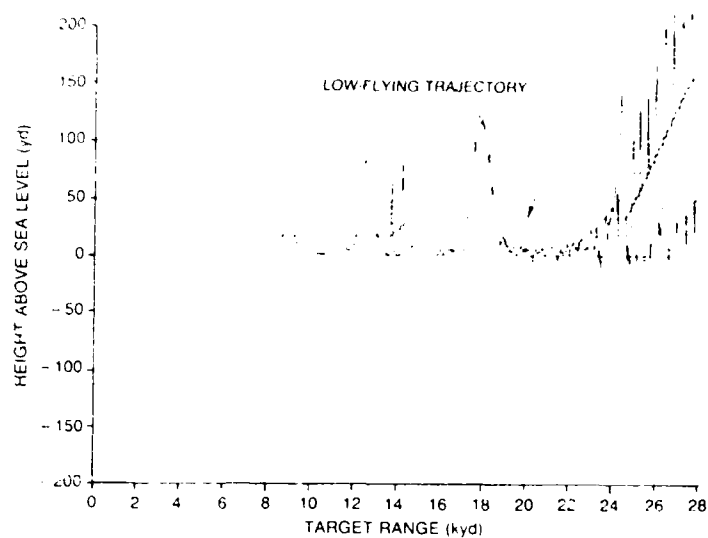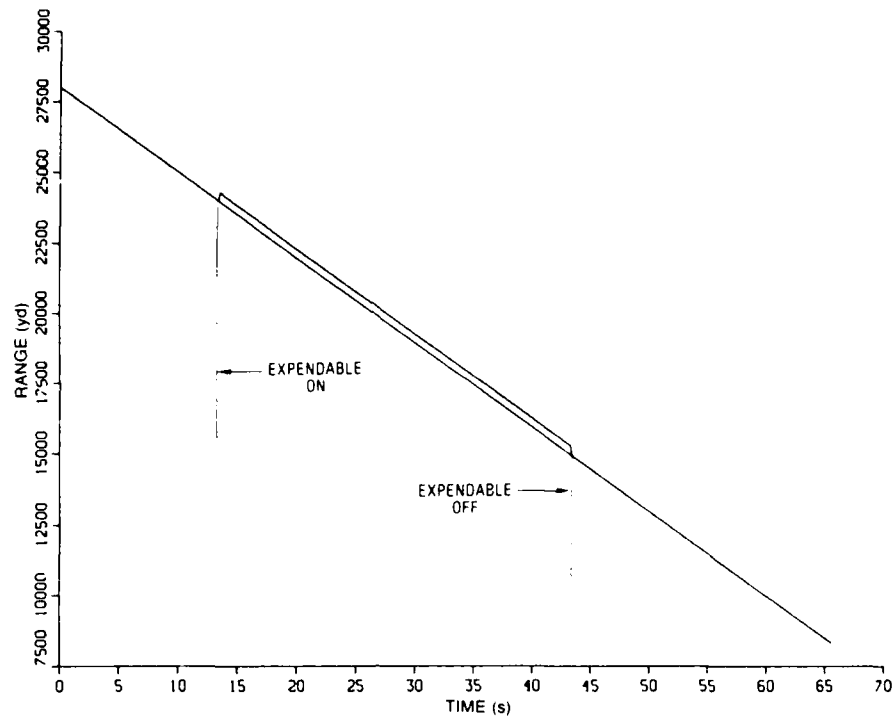
(a) Elevation tracking
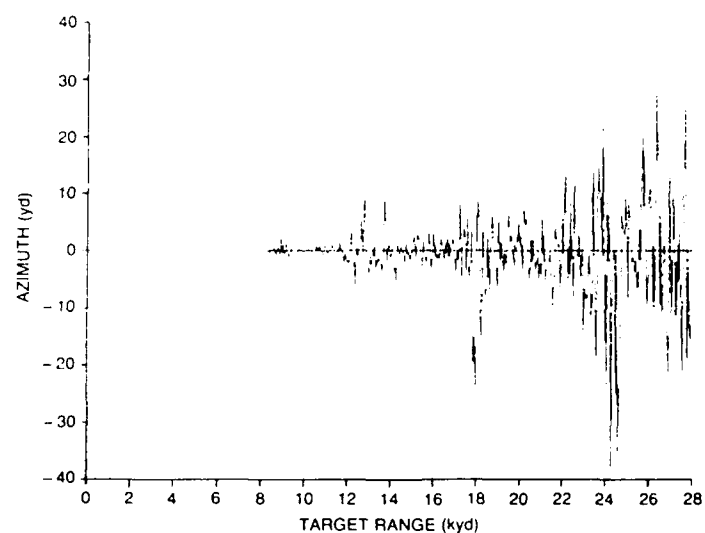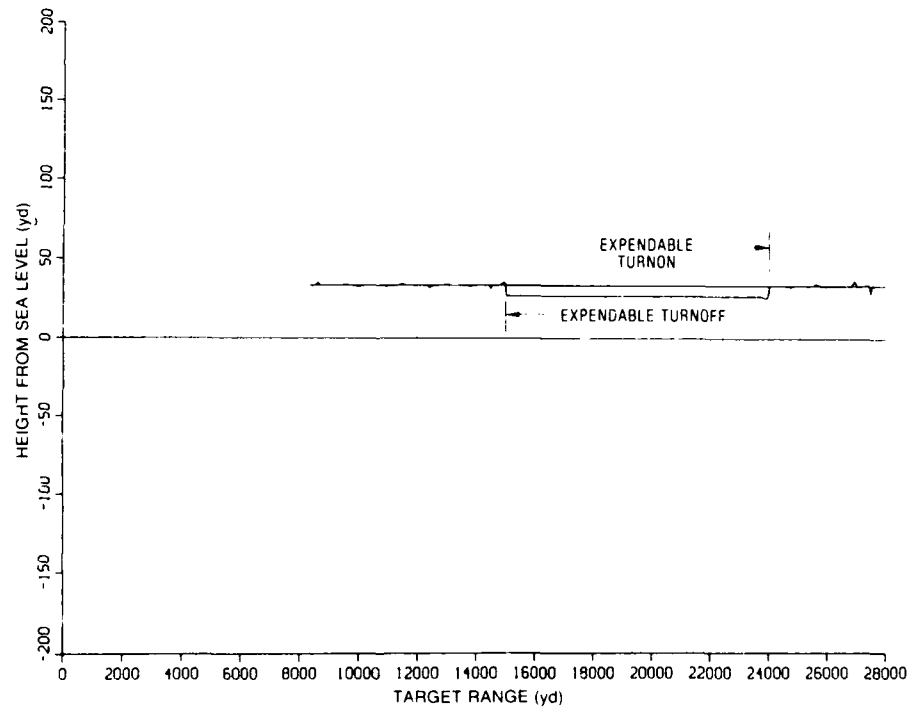

(b) Azimuth tracking

(c) Receiver gain

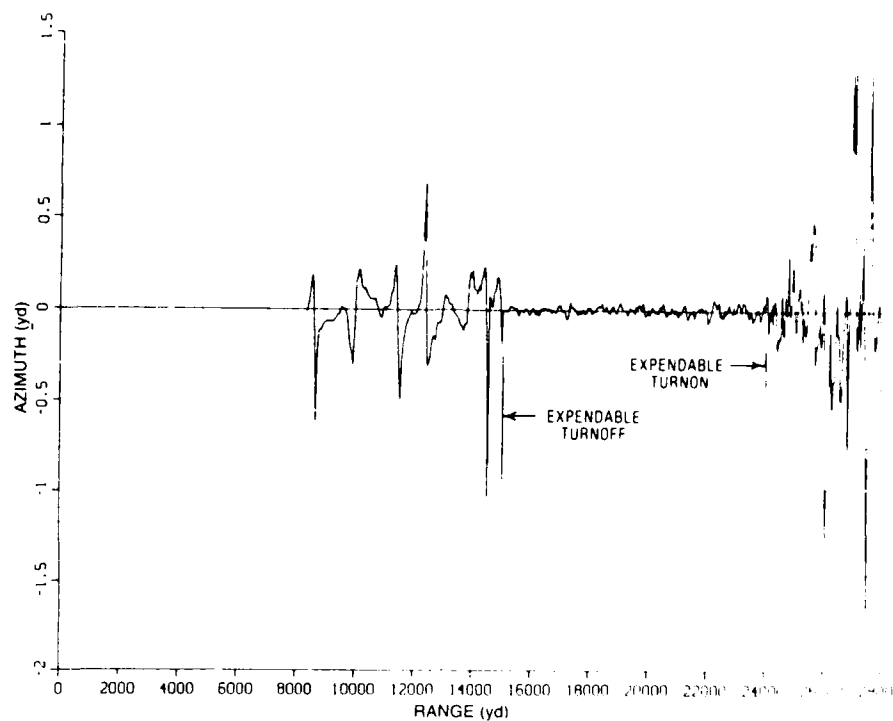Fig. 3 — A typical monopulse radar tracking
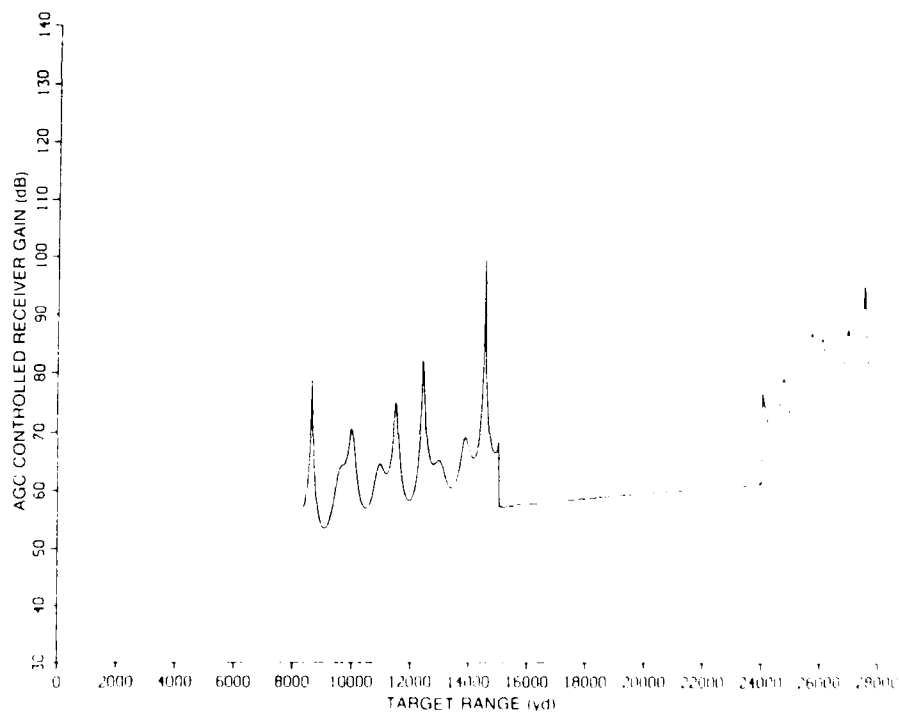
(a) Range tracking

(b) Elevation tracking

Fig. 4 — Monopulse radar tracking
for towed, expendable CM

(c) Azimuth tracking

(d) Signal level

Fig. 4 — (Continued) Monopulse radar tracking
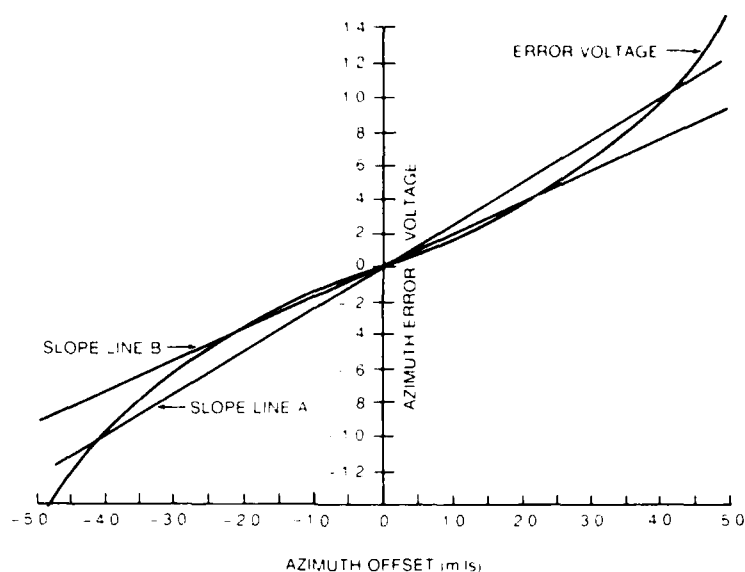for towed, expendable CM

Fig. 5 — Angle-error characteristics of a monopulse radar

To maintain a stable closed loop, the AGC system detects the peak voltage of the signal and provides a negative dc voltage to the IF amplifier. Assume the desired constant IF output voltage level is V. Then the IF amplifier gain, which is inversely proportional to the detected voltage, must be $V/\hat{V}_S$ or $R^2(t)V/\Sigma^2 \sqrt{P_t\sigma(t)}\ k$. Therefore the sum-signal and difference-signal IF outputs instantaneously coverage to

$$V_S = V \tag{2}$$

and

$$V_D = \frac{\Delta}{\Sigma}V, \tag{3}$$

which are then independent of the range and target scattering cross section. The overall closed-loop gain is thus a constant and is invariant with respect to time. If a dot-product angle-error detector is used, the angle-error voltage is $e = V^2(\Delta/\Sigma) \cos \theta$. Here θ is the relative phase between the sum- and difference-channel outputs, and the error voltage is proportional to the antenna difference pattern normalized by the sum pattern. This gives a nearly constant angle-error sensitivity vs signal level. It is time invariant if the AGC bandwidth is sufficiently large.

Figure 5 shows the typical nonlinear angle-error sensitivity measured by the AN/FPQ-6 radar with ~8 mils beamwidth [2] and two linear approximations. Line B provides a best fit for azimuth errors with ±3 mils, while line A is a best fit for errors up to ~±5 mils. For a small angle displacement, the voltage error may be considered linearly related to the antenna boresight error. A constant sensitivity, labeled K_1, is used in angle track throughout the report.
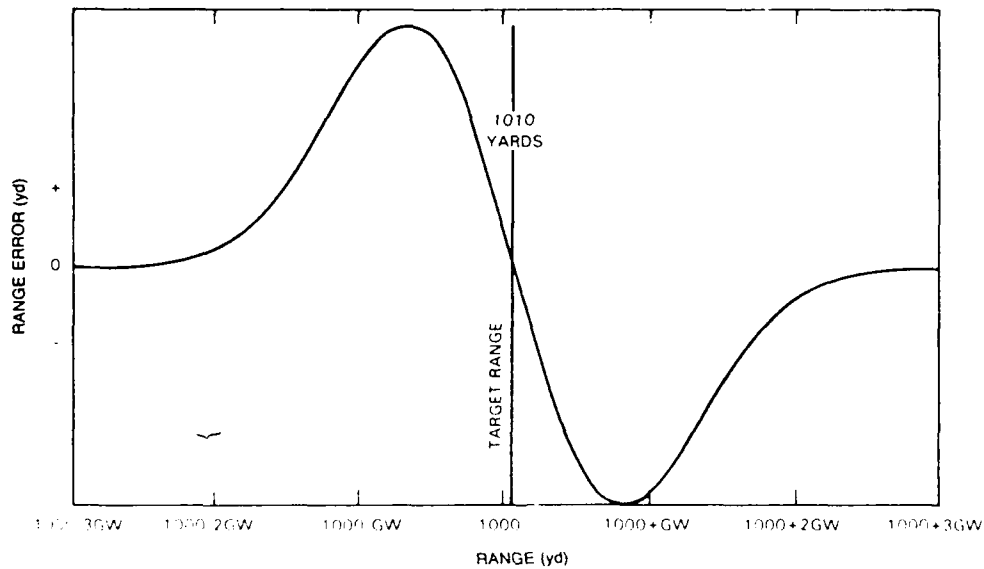
RANGE DISCRIMINATOR

A popularly used range discriminator is an early-late gate discriminator. The pulse shape is Gaussian with the pulse length equal to the gate length. The mathematical presentation of a range

7

discriminator is similar to that of an angle-error detector although their physical functionings are completely different. The discriminator output (Fig. 6(b)) is formed by the subtraction of the early and late gate integrator outputs, as shown in Fig. 6(a). The magnitude of the error signal obtained in Fig. 6(b) is a measure of the difference between the center of the gates and the center of the pulse. The sign of the error signal indicates the direction to which the range tracker has to move.
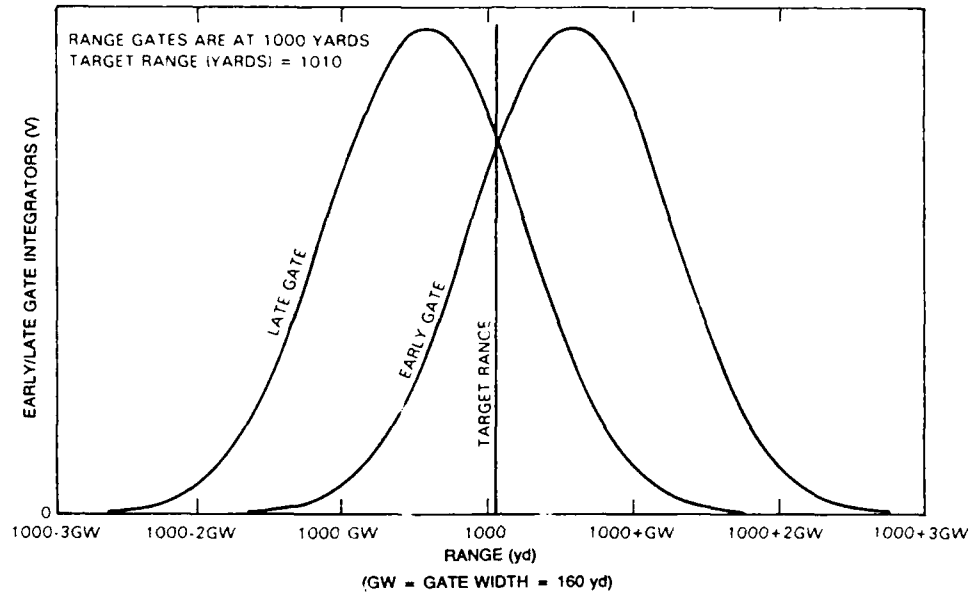
(a) — Early and late gate integrator outputs

(b) — Range discriminator output

Fig. 6 — Outputs

8

SERVO CONTROL AND SHAPING FILTER

Appropriate selections of bandwidth and loop gain are essential in designing a good servo control system. For a monopulse track radar, sufficiently wide AGC bandwidth is required to obtain a range- or time-independent angle-error sensitivity. Increasing the track open-loop beamwidth or reducing the closed-loop damping ratio generally increases the quickness of the servo control response and enhances its ability to closely follow a strong, steady signal. This is particularly desirable in a short-range target-tracking application in which target-angle scintillation errors are large. A wider servo bandwidth, however, allows more noise to pass through and causes erroneous motions of the tracking system. In practice, the bandwidth is limited to the minimum needed to maintain a reasonably small tracking lag error, although the optimum bandwidth is range-dependent. Proper selection of the overall loop gain, which may be constant or adaptive, is also necessary since it not only affects the track performance but also influences the system stability.

Let the servomotor be a simple integrator, represented by the transfer function K_2/s, where K_2 is a simplified constant factor affected by the amplifier gain and the motor torque and inertia. In the range tracker loop, K_2 may be a VCO gain factor. When modeling a tracking radar simulator with selectable angle-error sensitivity and servomotor constant, adding a shaping filter with flexible pole and zero placement is needed. The filter with a low-pass characteristic smooths out the IF angle-error voltage. It also shapes up the closed track loop, providing a desirable track performance.

In reference to electronic hardware implemented in the experimental TRAKX radar (tracking radar at K- and X-band) [3], a shaping filter represented by $(1 + \tau_2 s)/\tau_1 s$ is used here. A filter of higher order may be used later to include the antialiasing function.

ANGLE AND RANGE TRACKER LOOPS

As previously noted, the angle-track loop of a monopulse radar basically consists of an RF combining circuit, IF receiver with AGC, low-pass filter, and servomotor. They are primarily characterized by the angle-error sensitivity, poles and zeros of the shaping filter, and the servomotor integrator constant. Their transfer functions are described in the previous sections. These transfer functions are also applied to the range tracker loop with K_1 and K_2 indicating the range discriminator and VCO gain factor. A baseline model of Figs. 1 and 2 is described by Fig. 7.
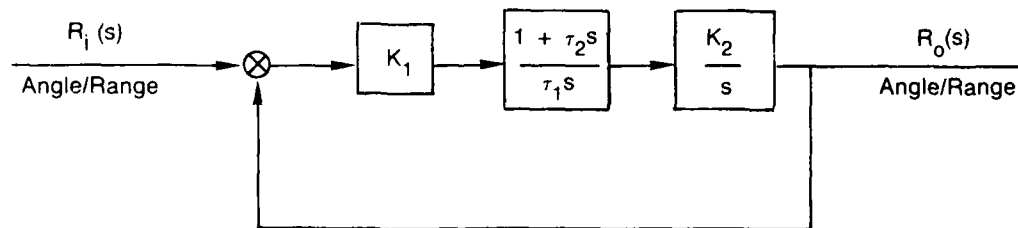

Fig. 7 — Baseline model of monopulse radar

The open-loop transfer function of the above signal-flow diagram is

$$G(s) = \frac{K_1 K_2 (1 + \tau_2 s)}{\tau_1 s^2}. \tag{4}$$

The gain crossover frequency, or the "open-loop bandwidth," can easily be calculated as

$$\omega_{OB} = \left[\frac{\dfrac{K_1^2 K_2^2 \tau_2^2}{\tau_1^2} + \sqrt{\dfrac{K_1^4 K_2^4 \tau_2^4}{\tau_1^4} + \dfrac{4K_1^2 K_2^2}{\tau_1^2}}}{2} \right]^{1/2}, \tag{5}$$

or, approximately

$$\omega_{OB} = \frac{K_1 K_2 \tau_2}{\tau_1}. \tag{6}$$

The negative corner frequency is $1/\tau_2$ (see Eq. (4)). It is good practice in most cases to have 10 dB magnitude at this corner frequency. As a measure of the loop stability, the phase margin is defined as $\underline{/G(j\omega_{OB})} - 180°$ and is consequently reduced to $\tan^{-1}(K_1 K_2 \tau_2^2/\tau_1)$ by Eqs. (6) and (4).

The open-loop Bode and Nyquist plots of Eq. (4) in angle track are shown in Figs. 8 and 9. The figures are plotted for the nominal case of $K_1 = 105.57$ V/rad, $K_2 = 0.087$ rad/sV, $\tau_1 = 0.1848$ s, $\tau_2 = 0.2521$ s. Determination of these parameters is discussed later. In the above case, the gain crossover frequency is calculated to be 2 Hz and the phase margin is 72.5°, which can also be obtained from Fig. 5 or Fig. 6.

To further understand track ability, we then consider the close-loop transfer function $R_o(s)/R_i(s)$ outlined in Fig. 7. It is easy to derive that

$$\frac{R_o(s)}{R_i(s)} = \frac{1 + \tau_2 s}{1 + \tau_2 s + \dfrac{\tau_1}{K_1 K_2} s^2}. \tag{7}$$

A "closed-loop bandwidth" can then be obtained, with Eq. (7) set to unity gain and solved for ω, that is,

$$\omega_{CL} = \sqrt{\frac{2K_1 K_2}{\tau_1}}. \tag{8}$$

More precisely, the loop bandwidth is defined as the frequency at which the gain has dropped to 70.7% of its zero frequency level. From Eq. (7), the angle or range output response for a step error-input response is $(1 + \tau_2 s)/s(1 + \tau_2 s + \tau_1 s^2/K_1 K_2)$. This can be partitioned into a more familiar form, i.e.,

$$R_o(s) = \frac{1}{s} - \frac{s}{\omega_n^2 \left[1 + \dfrac{2\zeta}{\omega_n} s + \dfrac{1}{\omega_n^2} s^2 \right]}, \tag{9}$$

with

$$\zeta = \frac{\tau_2}{2} \sqrt{\frac{K_1 K_2}{\tau_1}} \tag{10}$$

and

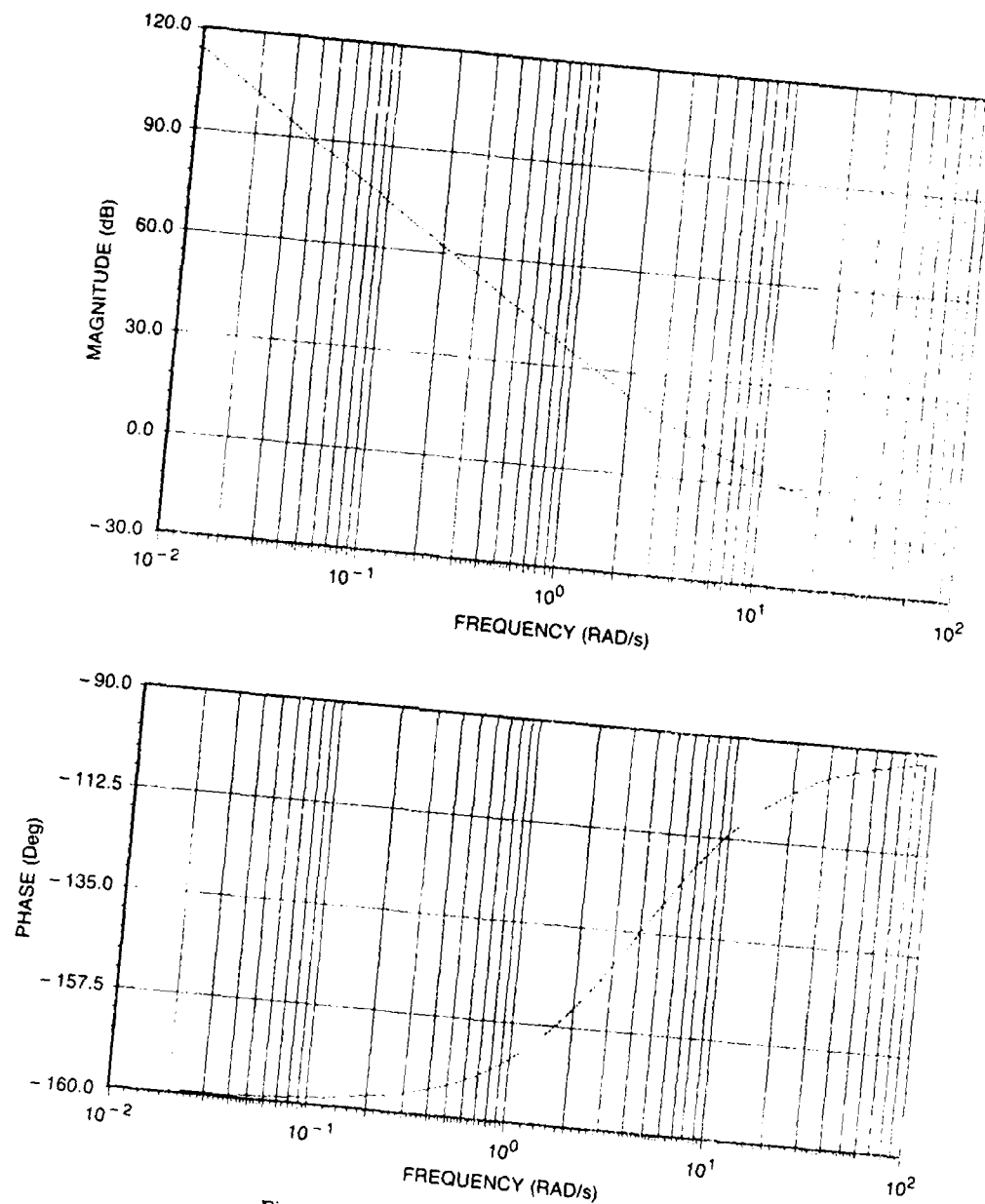$$\omega_n = \sqrt{\frac{K_1 K_2}{\tau_1}}.$$
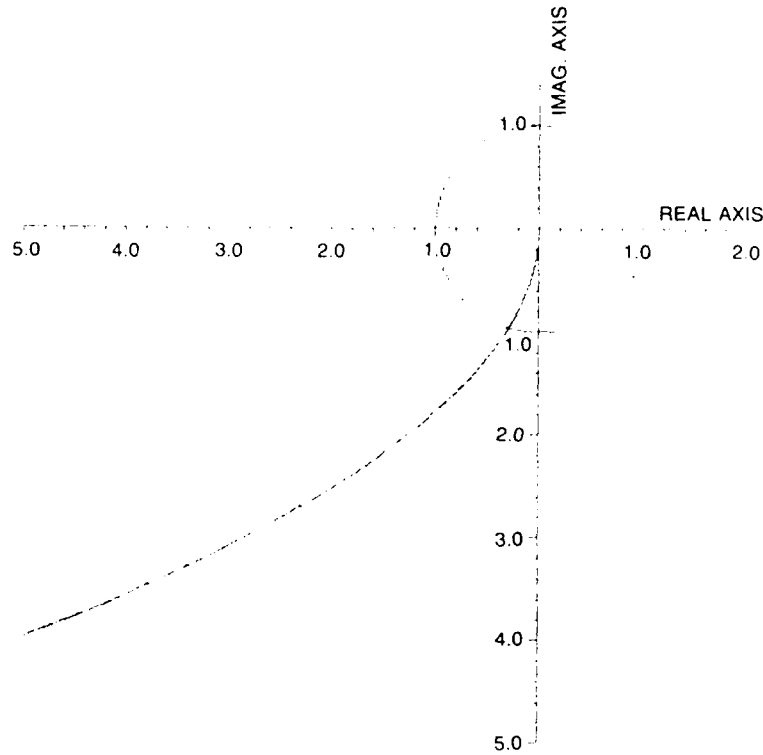
Fig. 8 — Bode plot of the angle-track loop

Fig. 9 — Nyquist plot of the angle-track loop

By combining Eqs. (6) and (10), the parameters τ_1 and τ_2 that must be determined in a shaping filter design can be expressed in terms of the damping ratio ζ, open-loop gain crossover ω_{OB}, and other radar parameters. As a result, $\tau_1 = 4K_1K_2\zeta^2/\omega_{OB}^2$ and $\tau_2 = 4\zeta^2/\omega_{OB}$. Furthermore, by taking the inverse Laplace transform of Eq. (9), an analytical solution describing the track loop response is obtained. For critical and underdamped cases,

$$r(t) = u(t) - \frac{1}{\sqrt{1 - \zeta^2}} e^{-\zeta\omega_n t} \sin\left(\omega_n \sqrt{1 - \zeta^2}\, t + \phi\right) \tag{11}$$

and

$$\phi = \tan^{-1} \frac{\sqrt{1 - \zeta^2}}{-\zeta},$$

and for the overdamped case,

$$r(t) = u(t) - \left[\frac{q_1}{q_1 - q_2} e^{q_1 t} - \frac{q_2}{q_1 - q_2} e^{q_2 t}\right] \tag{12}$$

with

$$q_1, q_2 = \omega_n\left(-\zeta \pm \sqrt{\zeta^2 - 1}\right).$$

12

Both the closed-loop frequency and step input transient responses for the nominal case are shown in Fig. 10. The loop bandwidth is ~1.59 Hz.
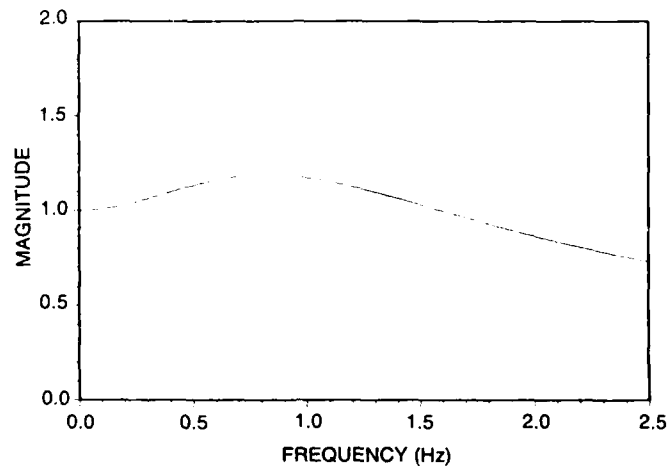

(a) — Closed-loop frequency
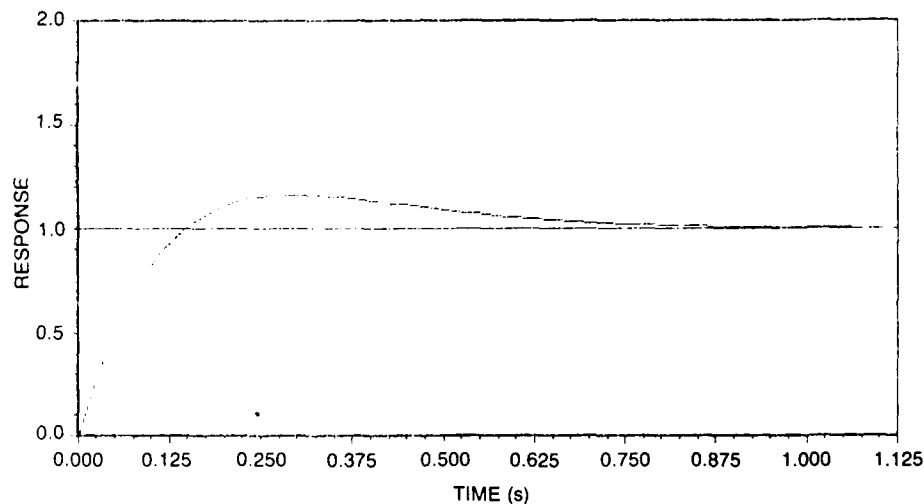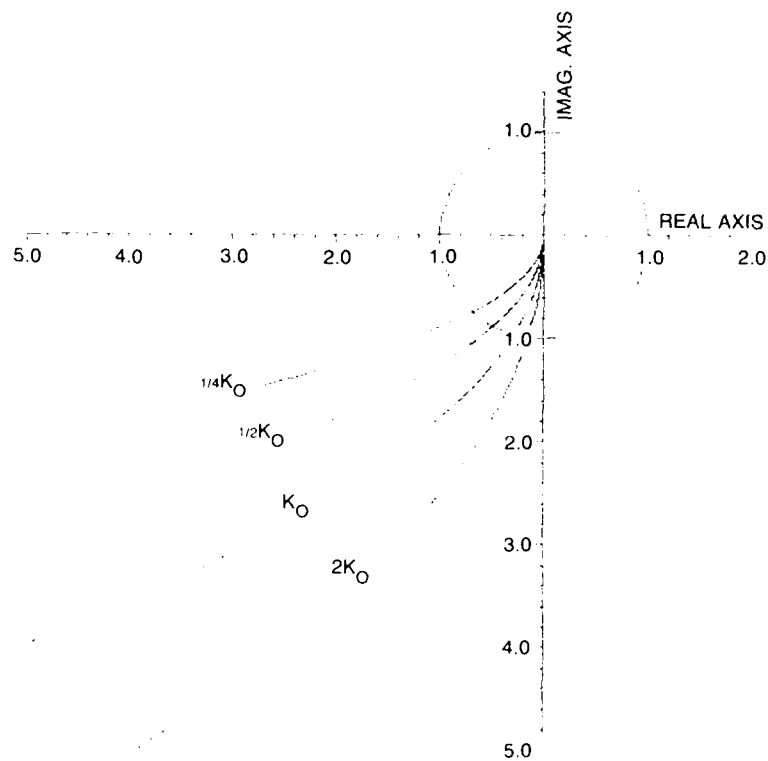

(b) — Step input transient

Fig. 10 — Response of the angle-track loop

MODEL SYNTHESIS AND TRACK PERFORMANCE

The baseline model (Eq. (4)) shows that the tracking control loop is relatively stable as long as the loop gain $K_o = K_1K_2/\tau_1$ is positive. This is shown in the Bode plots and in the Nyquist plots for various loop gains, with the frequency changing from 0 to 10^3 rad/s in Fig. 11(a) and from 0 to ∞ in Fig. 11(b). Since the multiplier K_1K_2 is time independent because of implementation of AGC, a wide range of τ_1 can be assigned to achieve a desirable loop bandwidth. Figure 12 shows that a decrease of the loop gain results in the decrease of loop bandwidth, hence, an increase is the track lag error. In the figure, oscillation gradually occurs because of the simultaneous reduction of the damping ratio affected by the decrease of the loop gain (see Eq. (10)).

13
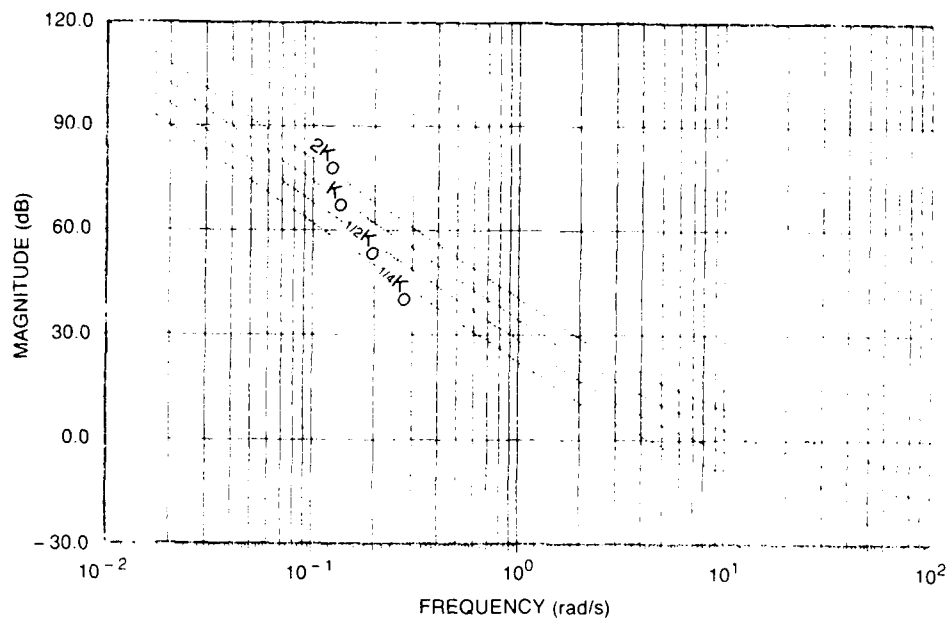
(a) — Bode plots
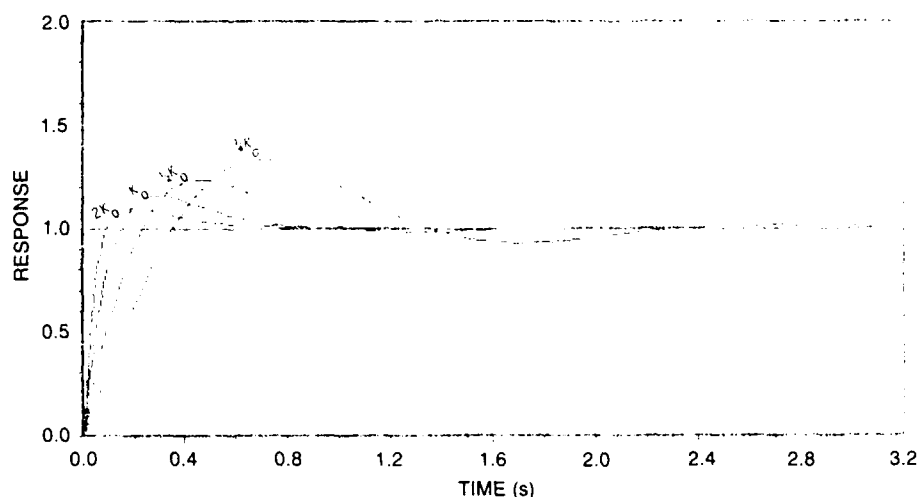

(b) — Nyquist plots

Fig. 11 — Loop gain plots

Fig. 12 — Step input transient response as a function of loop gains

In practice, it may be preferable to increase loop gain and simultaneously reduce τ_2 to obtain proper damping ratio without too much oscillation and overshoot (see Eq. (10)). Having determined proper damping ratio ζ and open-loop gain crossover frequency ω_{OB}, the filter pole/zero can easily be placed. This will result in a satisfactory angle track.

With the choice of $\zeta = 0.89$, Fig. 13(a) shows the closed-loop frequency responses for the gain crossover of $\omega_{OB} = 1, 2, 4$ Hz. In these cases, the closed-loop bandwidths are $\sim 0.8, 1.59, 3.18$ Hz. Figure 13(b) shows the corresponding step input transient responses.

For $\omega_{OB} = 2$ Hz, τ_1 and τ_2 can be placed at 0.084 and 0.115 s, 0.1848 and 0.2521 s, 0.37 and 0.51 s or 0.93 and 1.27 s, such that $\zeta = 0.6, 0.89, 1.26$, or 2, respectively. Figure 14 shows the Bode plots of these cases. Figure 15 shows the corresponding closed-loop frequency responses and the step input transient responses. The case that $\zeta = 0.89$, $\omega_{OB} = 2$ Hz, and the loop gain $K_o = 49.7$ is obviously preferable, this is being used as the baseline in the simulator development.

Similar arguments are applied to the range-tracker control loop. For practical applications, a Gaussian shaped pulse with a length of 160 yd 3 dB down from the peak is considered. This results in the discriminator constant factor $K_1 = 0.0069$ V/yd. Let $K_2 = 0.2$ yd/s·V as in Ref. 3. Then $\tau_1 = 4.43 \times 10^{-6}$ s and $\tau_2 = 0.1$ s must be designated for the shaping filter to give the range tracker the superior performance shown in Fig. 16. Figure 16 shows the closed-loop frequency response and the step input transient response. The range-tracker loop has a loop gain of ~ 312, open-loop gain crossover of 5 Hz, closed-loop bandwidth of 4 Hz, and damping ratio $\zeta = 0.89$.

By applying Eqs. (11) and (12), the angle error-input track responses can quickly be obtained with the plots shown in Fig. 17. for the cases $\omega_{OB} = 10$ Hz and $\zeta = 0.89$ (the nominal case), $\omega_{OB} = 50$ Hz and $\zeta = 0.89$, and $\omega_{OB} = 10$ Hz and $\zeta = 0.2$. This, on the other hand, validates those results obtained from a complex monopulse radar simulation. In that case, a 1°-beamwidth antenna, combining circuit, dot product detector, and early-late discriminator are modeled without simplification. The simulation is set to a special mode, a fixed-point target without electronic countermeasures (ECM) and multipath. The antenna boresight and range tracker are initially offset by 0.5° in elevation and azimuth, and by 100 yd in range. Figure 18 plots the track responses as a function of elapsed time. A comparison of Fig. 17 with Fig. 18 shows that the monopulse radar track performance resulting from complex model simulation is almost identical to that described by an analytical equation.

15
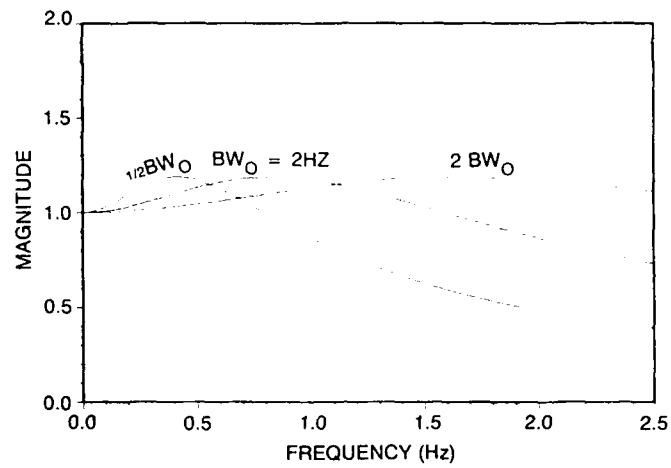
(a) — Closed-loop frequency responses
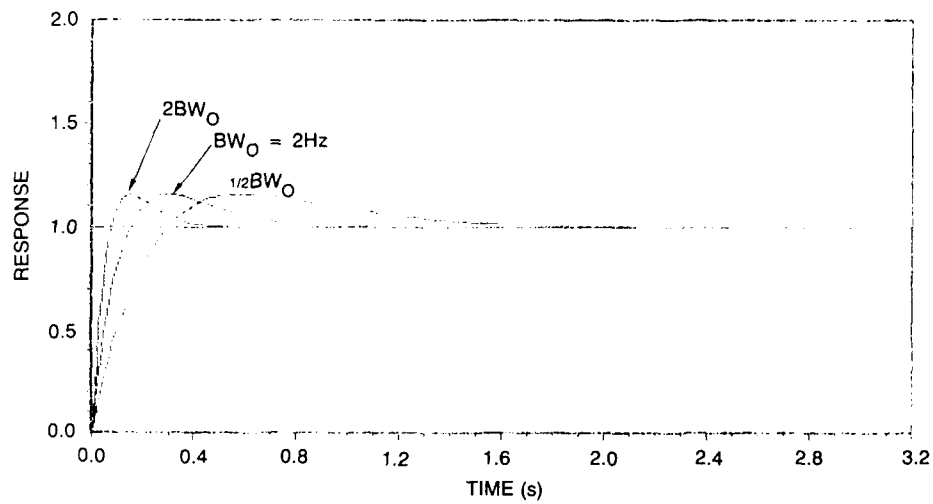
(b) — Step input transient responses

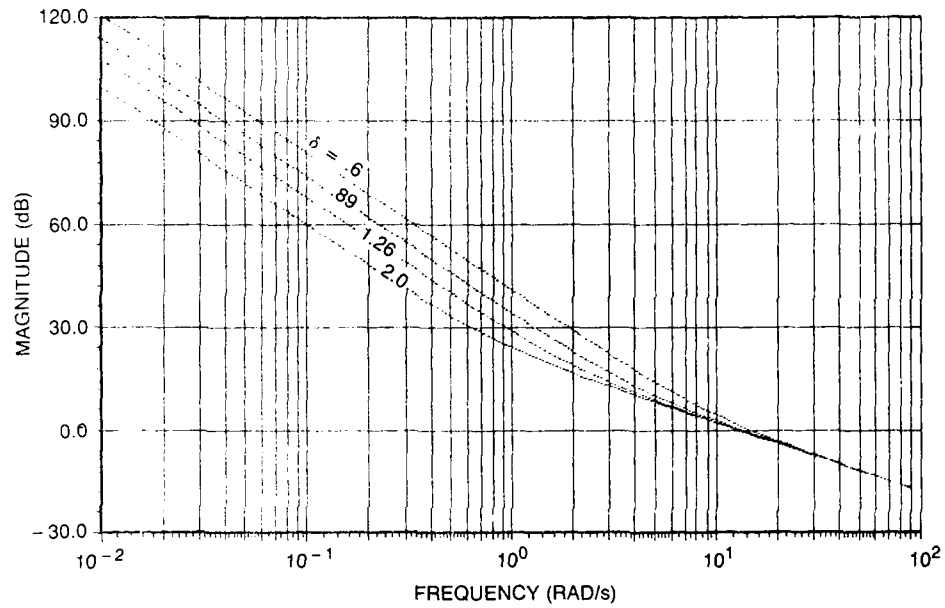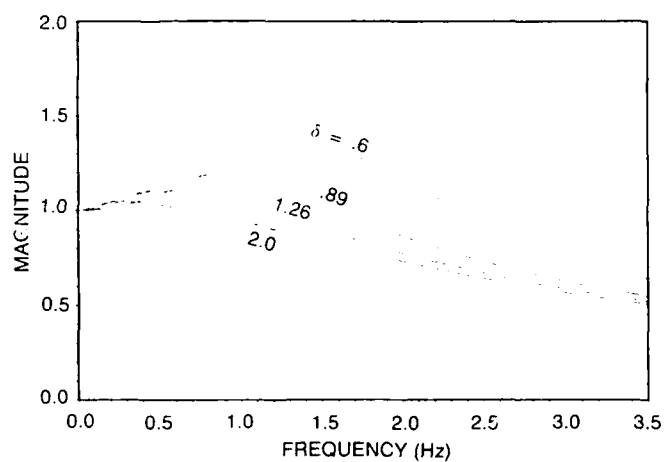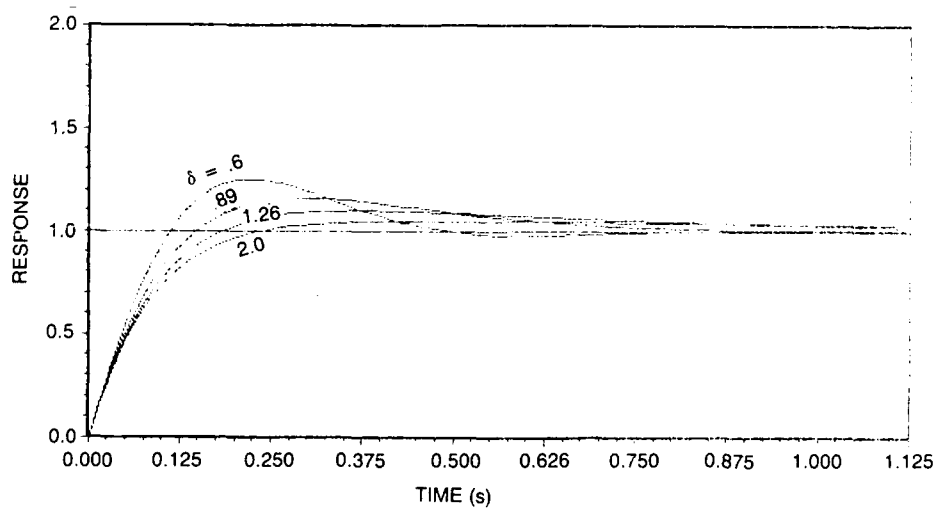Fig. 13 — Responses for various gain crossover frequencies

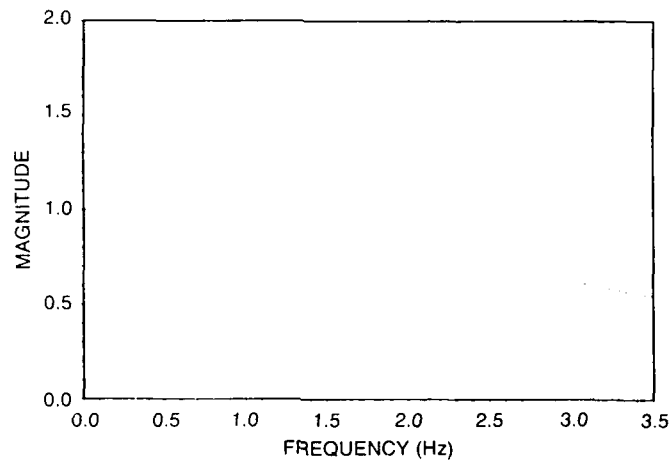Fig. 14 — Bode plots for the case of $\omega_{OB} = 2$ Hz and $\zeta = 0.6, 0.89, 1.26,$ and 2
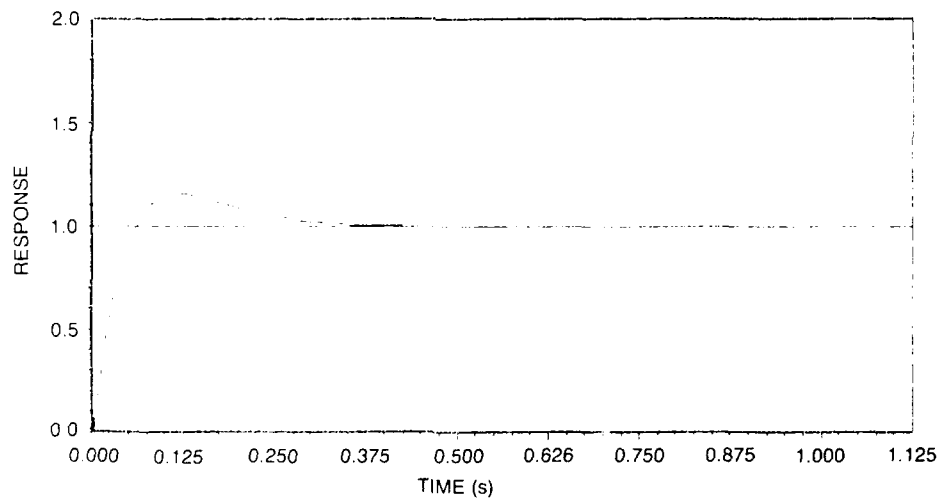
(a) — Closed-loop frequency

(b) — Step input transient

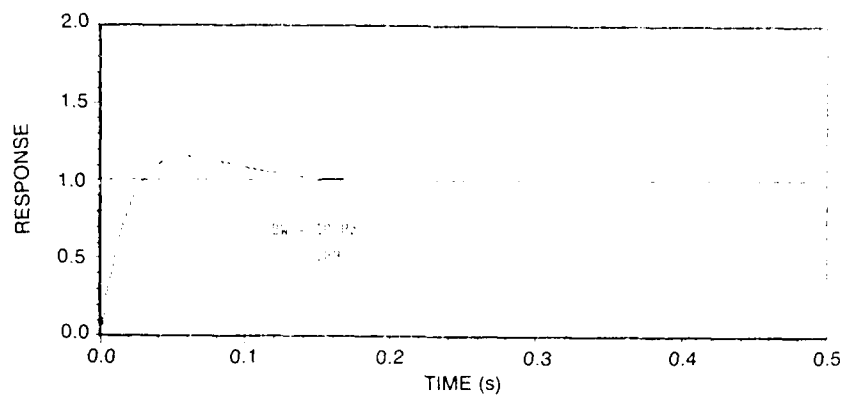Fig. 15 — Responses for the case of ω_{OB} = 2 Hz and ζ = 0.6, 0.89, 1.26, and 2
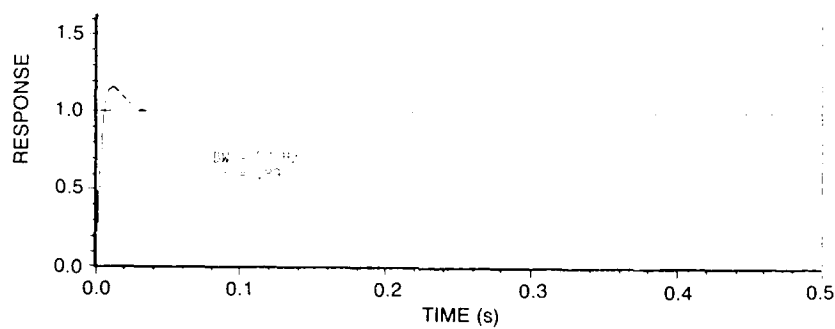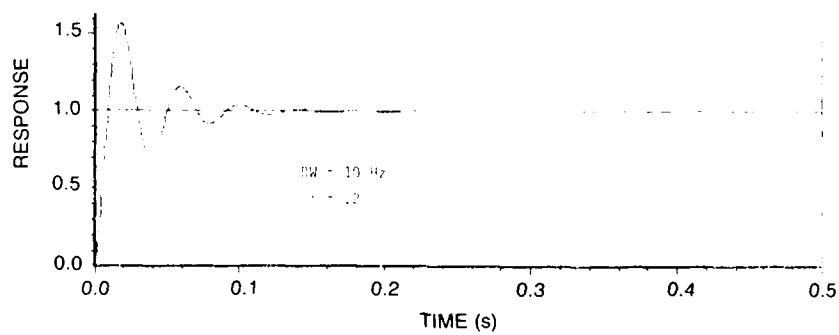
(a) — Closed-loop frequency

(b) — Step input transient

Fig. 16 — Response of the range tracker loop

(a) BW = 10 Hz, ζ = 0.89

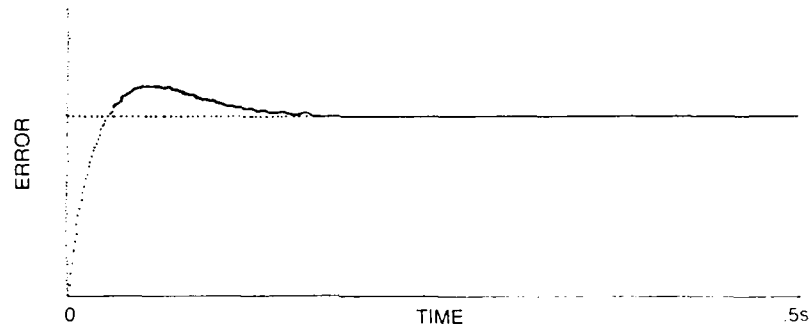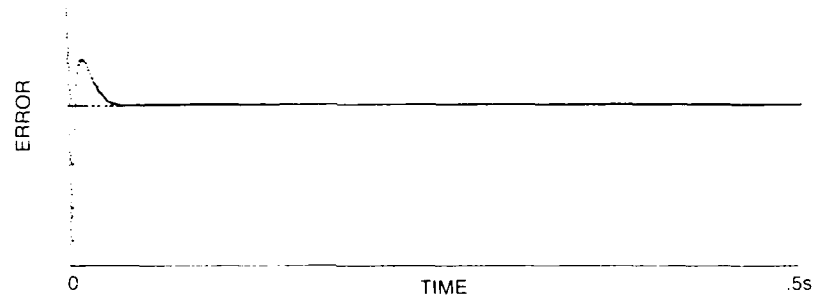(b) BW = 50 Hz, ζ = 0.89

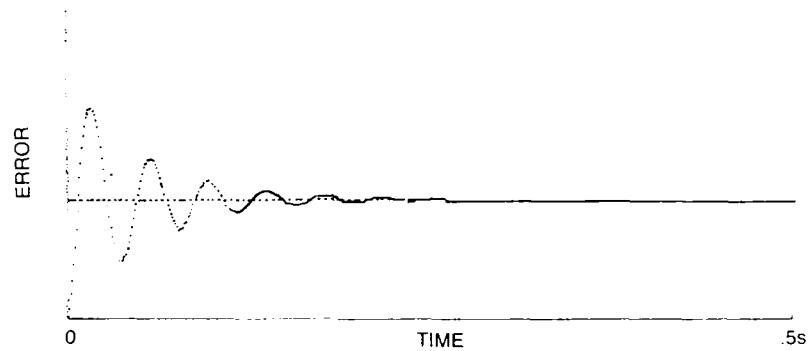(c) BW = 10 Hz, ζ = 0.2

Fig. 17 — Step input response

(a) BW = 10 Hz, ζ = 0.89

(b) BW = 50 Hz, ζ = 0.89

(c) BW = 10 Hz, ζ = 0.2

Fig. 18 — Transient responses of the corresponding cases of Fig. 17
(though model simulation)

CONCLUSIONS

A generic tracking radar model is being developed at NRL to provide realistic tracking performance on a finite-size complex target. The associated simulator can be used as a tool in synthesizing a monopulse radar and provides a means of assessing the effectiveness of monopulse countermeasures and counter-countermeasures in selectable tactical scenarios. It can also be used in identifying radar system peculiarity or physical limitations in radar design.

In this report, track performance considerations for monopulse radars are discussed from a theoretical viewpoint. By using a classical control approach, the radar tracking stability and sensitivity are analyzed in terms of the open-loop gain crossover, phase margin, closed-loop bandwidth, damping ratio, and natural oscillation frequency. Track loops are synthesized through filter pole/zero placement with the overall loop gain being considered. An analytical solution describing the angle and range tracking responses is also derived. This provides detailed insight into how basic radar characteristics affect monopulse radar track. Basic design of a monopulse radar or assessment of its fundamental track performance can also be accomplished without performing a time-consuming simulation. Within the framework discussed here, further monopulse radar modeling of relative complexity, either through computer simulation or theoretical analysis, can easily be done.

REFERENCES

1. S.M. Sherman, *Monopulse Principles and Techniques* (Artech House, Norwood, MA, 1984).

2. "Final Report—Measurements and Analysis of Performance of MIPIR-Missile Precision Instrumentation Radar Set AN/FPQ-6," RCA Report under Contract NOW 61-0428d, Dec., 1964

3. D. Cross, D. Howard, M. Lipka, A. Mays, and E. Ornstein, "TRAKX: A Dual-Frequency Tracking Radar," *Microwave J.* **19** (9), 39-41 (1976).